

Atmospheric influence on lithosphere formation during cooling of a global magma ocean

Influencia atmosférica en la formación de la litosfera durante el enfriamiento de un océano magmático global

Miguel Ángel Carapia-Pérez^{1,*}, Edgardo Cañón-Tapia¹

¹ División de Ciencias de la Tierra, Centro de Investigación Científica y de Educación Superior de Ensenada, Carretera Ensenada, Tijuana No. 3918, Zona Playitas, CP. 22860, Ensenada, B.C. México.

* Corresponding author:
(M.A. Carapia Pérez) mcarapia@cicese.edu.mx

How to cite this article:

Carapia-Pérez, M.A., Cañón-Tapia, E., 2025, Atmospheric influence on lithosphere formation during cooling of a global magma ocean: Boletín de la Sociedad Geológica Mexicana, 77(1), A021124. <http://dx.doi.org/10.18268/BSGM2025v77n1a021124>

Manuscript received: April 9, 2024
Corrected manuscript received: September 10, 2024
Manuscript accepted: September 13, 2024

Peer Reviewing under the responsibility of Universidad Nacional Autónoma de México.

This is an open access article under the CC BY-NC-SA license (<https://creativecommons.org/licenses/by-nc-sa/4.0/>)

ABSTRACT

The history of the cooling and solidification of the magma ocean produced after the large Moon-forming impact on Earth remains ill-constrained. The most commonly accepted scenario invokes a greenhouse effect of the atmosphere preventing the formation of a solid lithosphere before the complete solidification of the magma ocean from below. In this work we reexamine the cooling history of the planet after the impact, solving the 1D heat diffusion equation in spherical coordinates using the pdepe solver of Matlab for different atmospheric conditions that are compatible with a large impact event. Lithosphere formation is constrained by the time it takes for the atmosphere to drop below 1400°K when the conditions are adequate for solidifying a peridotite melt. Our results indicate that the Earth could have had a different thermal evolution than what has been commonly considered until now in most models of Earth's evolution.

Keywords: magma ocean, thermal model, atmosphere, early Earth.

RESUMEN

La historia de enfriamiento y solidificación del océano de magma producido después del gran impacto de la formación de la Luna en la Tierra continúa incierta. El escenario más ampliamente aceptado invoca un efecto invernadero de la atmósfera que impide la formación de una litosfera sólida antes de que el océano de magma se solidifique por completo desde abajo. En este trabajo re-examinamos la historia de enfriamiento del planeta después del impacto resolviendo la ecuación de difusión de calor 1D en coordenadas esféricas utilizando el solucionador pdepe de Matlab para diferentes condiciones atmosféricas que son compatibles con un evento de gran impacto. La formación de litosfera está limitada por el tiempo que tarda la atmósfera en descender por debajo de los 1400°K cuando las condiciones son adecuadas para la solidificación de una peridotita fundida. Nuestros resultados indican que la Tierra podría haber tenido una evolución térmica diferente a la que comúnmente se ha considerado hasta ahora en la mayoría de los modelos de evolución de la Tierra.

Palabras clave: océano de magma, modelo térmico, atmósfera, Tierra primitiva.

1. Introduction

The thermal energy released by a giant collision similar to that thought to be responsible for the formation of the Earth-Moon system could have triggered the formation of a magma ocean at the surface of the Earth (Tonks and Melosh, 1993). Numerical models of similar collisions show temperatures so high that they cause the evaporation of silicates (Canup, 2008).

In addition, the fall of the small fragments that remained orbiting within the Roche limit contributed to the increase in surface temperature (Carter *et al.*, 2020). For these reasons, the formation of a global magma ocean covering Earth's surface following a high-energy impact is considered an almost inevitable consequence.

Details of how the magma ocean solidified after impact are uncertain. The most accepted model for Earth is that the magma ocean cooled from its bottom towards the surface, eventually leading to the formation of the lithospheric cover (Elkins-Tanton, 2012; Labrosse *et al.*, 2007; Solomatov, 2015; Zhang *et al.*, 2022). Such a conclusion is reached by considering that the magma ocean's cooling occurred due to adiabatic behavior and large-scale mantle circulation. Another key aspect of these models is the role of greenhouse warming in sustaining elevated surface temperatures on early Earth, which inhibited the cooling and solidification of the magma ocean from the surface downward. However, the extent to which the atmosphere can influence the heat flow behavior of the magma ocean during its cooling has not been evaluated in detail.

The early Earth's atmosphere was likely determined by an interplay between volatile delivery, outgassing, and atmospheric erosion (Schlichting and Mukhopadhyay, 2018). Such an atmosphere may have originated from the gradual release of volatiles during the accretion of meteorites in the early stages of planetary formation. In the canonical Moon-forming impact, only around 10% of the atmosphere would have been lost from the immediate effects of the collision, but atmo-

spheric mass loss is sensitive to the details of the impact scenario (Kegerreis *et al.*, 2020). Because the canonical model is not a unique solution, and the formation of the Moon could have occurred in a range of velocities and impact angles (Čuk and Stewart, 2012), the possibility that the early atmosphere could have been lost almost entirely, due to the great impact that gave rise to the Moon, remains viable.

Given the uncertainties concerning the very existence of an atmosphere just after a large impact event, the form in which its existence could have affected the formation of a lithosphere remains open for discussion. In this work, we explore the possible influence of the atmosphere in the cooling conditions of an Earth-like planet from post-impact-like conditions using a thermal model. Our results allow us to identify the threshold value of atmospheric heat transfer necessary to enable the cooling of the magma ocean either from above or from beneath the surface. Recognizing the conditions that promote lithospheric formation prior to the solidification of the deeper portions of a global magma ocean is essential for a better understanding of the planet's early evolution.

2. Materials and Methods

2.1. CHARACTERISTICS OF THE MODEL

We developed a one-dimensional model in MATLAB that solves the heat diffusion equation in spherical coordinates. We defined concentric layers based on the present-day internal structure of the Earth, incorporating certain simplifications. The core was considered as a single undifferentiated mass. The rest of the planet was considered part of the mantle, which was divided into an outer mantle and an inner mantle according to their initial temperatures. The top of the upper mantle is where a solid lithosphere is expected to be formed if the temperature of that surface falls below a threshold value, so there is no need to introduce an extra layer to describe the upper

boundary in the initial steps of the modeling.

Once a lithospheric layer is formed, the thermal properties of the upper layer need to be adjusted accordingly. Above the mantle, we included an outer layer in our model representing the atmosphere. The temperature beyond our atmospheric layer was equal to that of outer space.

2.1.1. INITIAL TEMPERATURES

In our model, the initial temperatures are constant in each of the layers, including the atmosphere (Figure 1). The initial temperatures of our model are based on the results of a smoothed particle hydrodynamics (SPH) simulation (Canup, 2008). Figure 1a illustrates the thermal results of a collision with the canonical impact model (Canup, 2008) and the temperature profiles that we used as initial conditions in our models. The temperature profiles of the silicates after impact are shown in blue and those of iron components in red in Figure 1a. The orange and green lines are the temperature profiles we use to constrain initial maximum and minimum temperatures for modeling. Although these lines are not the exact envelopes of the thermal results of the collision, they are representative of the maximum and minimum temperatures of most of the fragments that were accreted to form the Earth. Those profiles are shown as the red and blue lines, respectively, in Figure 1b.

The atmosphere temperatures of 2000 and 4000 K were chosen because they are reasonably expected values after a large collision, in addition to being the most used in previous works (*e.g.*, Nakazawa *et al.*, 1985; Abe, 1993; Canup and Esposito, 1996; Sleep *et al.*, 2001; Zahnle, 2006; Zahnle *et al.*, 2007). All the values used during the modeling are shown in Table 1.

2.1.2. HEAT TRANSFER

The balance between the heat generated in the formation of the Earth and the heat released into space allows us to understand its thermal evolution (Hofmeister, 2020). Heat transfer can occur

through three different mechanisms: conduction, radiation and convection. Radiation is the emission of energy in the form of electromagnetic waves from surfaces of finite temperature, which can travel through a vacuum.

Conduction is the transfer of energy within a medium through the movement and interaction of particles. As constantly happens when nearby molecules collide, a transfer of energy in the direction of decreasing temperature must occur. The random molecular motion that causes the net transfer of energy can be seen as energy diffusion.

Finally, convection is the transfer of heat through two different mechanisms, diffusion and advection. Advection is the movement of the fluid and diffusion allows the transfer of energy by molecular movement (Incropera *et al.*, 2007). It is necessary to clarify that the movement of the material does not imply the transfer of heat, but the way in which a greater quantity of particles of abundant energy make contact with particles of lower energy. In the presence of a temperature gradient, the movement of the material contributes to heat transfer. That is, convection can be considered as conduction favored by movement (Çengel, 2006).

In general, heat flow is proportional to the temperature differences between two locations, flowing from areas with higher heat to those with lower heat. This always happens regardless of the heat transport mechanism. Thus, heat transport by the different mechanisms can be described using the following expressions (Incropera *et al.*, 2007):

$$q_{rad} = h_{radiative} (T_2 - T_1) \quad (1a)$$

$$q_{cond} = -k \frac{dT}{dx} = -\frac{k}{L} (T_2 - T_1) \quad (1b)$$

$$q_{conv} = h_{convective} (T_2 - T_1) \quad (1c)$$

Equations (1) show on the left side the heat flow for each mechanism. On the right side, a proportionality constant (depending on the heat transport mechanism) multiplies the temperature difference

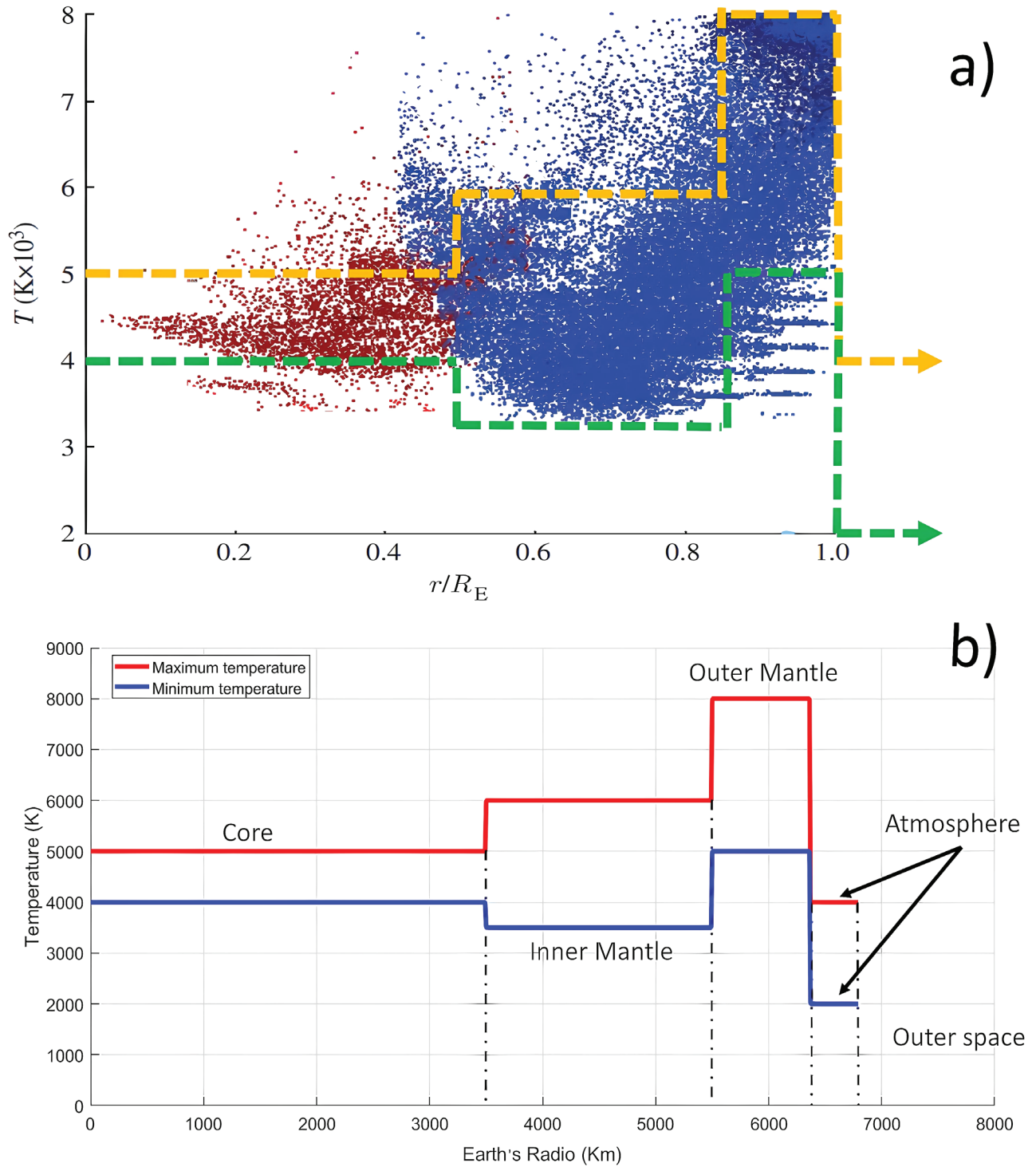


Figure 1 a) temperature in the proto-Earth as a function of depth (where r is the distance from the planet's center and R_E 6378 km) from Canup (2008). Red and blue points show the original proto-Earth material at the simulation's final time step (31 h), while dark blue points (upper right) are silicate particles originating from the impactor that are accreted by the proto-Earth. The green and orange lines are the temperature profiles we use to constrain initial maximum and minimum temperatures for our model. Those profiles are shown in b) without the points from the SPH simulation.

between two places. Heat flow will occur in any medium or between media where there is a temperature gradient. The proportionality constant depends on the particular mechanism; in equation 1a, $h_{\text{radiative}}$ is associated with the Stefan Boltzmann constant and the surface emissivity. In equation 1b, thermal conductivity is the material property that determines the speed of heat transfer. In equation 1c, $h_{\text{convective}}$ depends on the characteristics of the material, the type of convection or the phase changes it may experience.

Equations (1) have the same general form because “heat transfer (or heat) is thermal energy in transit due to a spatial temperature difference” (Incropera *et al.*, 2007). Thus, regardless of the details of the mechanism of transport, heat transfer can be modeled with the appropriate choice of the proportionality constant. This proportionality constant is known in engineering as effective thermal conductivity. Its numerical value can be expressed as a multiple of the thermal conductivity of the material being modeled (see below). Although this approximation cannot be used to appreciate the mechanical aspects of convection (*i.e.* the displacement of the fluid involved), it provides a solid argument in relation to its thermal effects.

2.1.1.3. HEAT EQUATION

Our model uses the heat diffusion equation to calculate the temperature as a function of radial distance from the center of the planet. In general, the heat diffusion equation can be written as:

$$\frac{\partial T}{\partial t} = \frac{1}{r^2} \alpha \frac{\partial}{\partial r} \left(r^2 \frac{\partial T}{\partial r} \right) + R \quad (2)$$

where α is thermal diffusivity, T is temperature, t is time, R includes the external heat sources and r is the radius of a sphere. During the magma ocean phase modeled in this work, the radiogenic heat production rate (R) is negligible, and therefore it could be excluded from the calculations without affecting the main conclusions (see appendix A). Nevertheless, for the sake of completeness, the influence of this term is considered below.

Thermal diffusivity is defined in terms of the thermal conductivity (k) and the product of the specific heat of the body (Cp) and its density (ρ): $\alpha = k/(Cp*\rho)$. Diffusivity measures the ability of a material to conduct thermal energy relative to its ability to store thermal energy (Incropera *et al.*, 2007). When the diffusivity is small the material has a slow response to energy transfer; a large diffusivity has a fast response to heat transfer (Hofmeister and Criss, 2019; Hofmeister, 2020). Thus, thermal diffusivity governs how quickly thermal fields change, while thermal conductivity describes the amount of thermal energy that moves down a thermal gradient (Whittington, 2019; Hofmeister, 2020).

The radiogenic heat production rate is calculated with equation 3, using the parameters from Chapter 2 in Hofmeister (2020).

$$R = 3.51 * 10^{-3} \xi_{K,ppm} e^{0.5543t} + 0.0263 \xi_{Th,ppb} e^{0.0495t} + \xi_{U,ppb} [0.0943 e^{0.1551t} + 0.00421 e^{0.9849t}] \quad (3)$$

$\xi_{K,ppm}$, $\xi_{Th,ppb}$ and $\xi_{U,ppb}$ are the present-day concentrations of the bulk elements in the rock in the indicated units. t is the age of interest. In the present work, the production of heat by radiogenic elements is homogeneously distributed throughout the mantle and R is reported as picowatts per kg of rock.

2.1.1.4. EFFECTIVE THERMAL CONDUCTIVITY

During the magma ocean phase on Earth, after the impact, the planet was most likely completely molten due to the high temperatures that were reached (Tonks and Melosh, 1993; Canup, 2008). Estimating a specific thermal diffusivity for this early period on the planet is difficult. Nevertheless, as a first approximation, we can use an effective thermal conductivity capable of representing the effects of the convective movement of the mantle. Effective thermal conductivity has been used before to model convection during magma ocean solidification with novel results (Monteux *et al.*, 2016; Monteux *et al.*, 2020). In our case,

Table 1. Thermal properties used in simulations.

Property	Range	Symbol	Units	References
Mantle density	3500	ρ	kg / m ³	Suzuki and Ohtani (2003)
Atmosphere density	1	ρ	kg / m ³	Incropera <i>et al.</i> (2007)
Core density	11000	ρ	kg / m ³	Melchior (1986)
Mantle thermal conductivity	3.6	k	W / (m K)	Goncharov <i>et al.</i> (2009)
Atmosphere thermal conductivity	0.05	k	W / (m K)	Incropera <i>et al.</i> (2007)
Core thermal conductivity	100	k	W / (m K)	Melchior (1986)
Mantle specific heat	1000	Cp	J / (kg K)	Solomatov (2015)
Atmosphere specific heat	2000	Cp	J / (kg K)	Incropera <i>et al.</i> (2007)
Core specific heat	700	Cp	J / (kg K)	Melchior (1986)
Mantle k convective	10 ² – 10 ⁵	k_{conv}		
Atmosphere k convective	10 ² – 10 ⁵	k_{conv}		

a first order approximation of the effect of an atmosphere on the temperature of the upper part of the cooling mantle was obtained by considering an effective thermal conductivity, along with engineering applications for heat exchangers (*e.g.*, Incropera *et al.*, 2007; Lienhard and Lienhard, 2008; Çengel, 2006).

In engineering, the simplest way to visualize the complex convective cooling part of a system is to consider the heat transfer of the whole system through thermal resistance to heat transfer (Incropera *et al.*, 2007; Lienhard and Lienhard, 2008; Çengel, 2006). The entire fluid is thus considered a single layer of a highly conductive material because heat is transported very efficiently in a convective fluid.

To simulate the higher efficiency of heat transfer in a convective medium relative to that of a conductive medium in equation (2), it suffices to introduce a numerical factor, larger than 1, that multiplies the thermal diffusivity. We call that factor k_{conv} , to emphasize the fact that it is a numerical factor introduced to simulate the thermal effects of a more efficient mechanism of heat transport such as that of convection.

Nevertheless, it must be remarked that such a numerical factor does not have dimensions.

To obtain a numerical value of k_{conv} that can represent liquid convection in the mantle we use the Nusselt number in analogy with heat exchangers. In other words, $k_{conv} = Nu$, where Nu is calculated according to the equation $Nu = 0.164 * Ra^{0.337}$ (Wolstencroft *et al.*, 2009). Ra is the Rayleigh number and can be defined as $Ra = (\beta \rho g L^3 \Delta T) / (\eta \alpha)$.

By substituting likely values for a magma ocean from Solomatov (2015) of thermal expansion $\beta = 5e-5$ (1/K), gravity acceleration $g = 9.8$ (m/s²), viscosity of melt at liquidus $\eta = 0.1$ (Pa s), thermal diffusivity is $\alpha = k / (Cp * \rho)$ with $Cp = 1000$ (J/kg*K) and $k = 3.6$ (W/m*K) from Goncharov *et al.* (2009) and melt density $\rho = 3500$ (kg/m³ from Suzuki and Ohtani (2003)), and adopting values from the largest initial temperature difference $\Delta T \sim 2000$ K and using the principal resolution of our model point grid $L \sim 10$ km, we obtain a value of $Ra \sim 6.8e+17$ and $Nu \sim 1.5e+05$. Therefore, it is reasonable to adopt the value of $1e5$ as the upper limit of k_{conv} . We also explore the thermal effects of less efficient convection, setting as a minimum value for k_{conv} $1e2$.

In other words, in our model, we are considering the possibility that liquid convection transmits heat between 100 and 100000 times more efficiently than the solid thermal conductivity of the mantle.

2.1.5. SOLIDIFICATION THRESHOLD

As cooling proceeds, the solidification of the magma ocean is eventually reached. The solidification process not only changes the rheological properties of the material, but also influences its thermal properties. Thus, the solidification process needs to be included in our simulations. We choose the solidus and liquidus curves used by Nikolaou *et al.* (2019) to differentiate the physical state of the mantle at the beginning of the formation of the lithosphere. These curves (described by the author as “synthetic”) have been calculated for peridotite at different mantle pressures (P). They employ data from multiple studies. For the solidus they use data from Hirschmann (2000) for $P \in [0, 2.7]$ GPa, Herzberg *et al.* (2000) for $P \in [2.7, 22.5]$ GPa, and Fiquet *et al.* (2010) for $P \geq 22.5$ GPa, while for the liquidus, the data are from Zhang and Herzberg (1994) for $P \in [0, 22.5]$ GPa and from Fiquet *et al.* (2010) for $P \geq 22.5$ GPa.

To model the change in the conditions of heat flux occurring as the result of solidification, we use a linear decrease of the thermal conductivity of the material that is at a temperature between the solidus and liquidus. The thermal conductivity of the solid mantle material was fixed at 3.6 W/m K (Goncharov *et al.*, 2009). The conductivity of the purely liquid phase was the effective conductivity, k_{conv} , as explained above. We are aware that the thermal effects of crystallization are not linear, but tend to display a drastic jump once a critical crystallinity percentage has been reached. Thus, our approximation overlooks details in the path followed by the percentage of molten material. However, the main differences are found in the intermediate percentages of solidification (40-60%) where the jump in thermal and rheological properties takes place. In addition, the linear

approximation is easier to use computationally and favors the stability of the numerical calculations, which allows us to evaluate a large number of simulations in a short time. Thus, we consider that the balance between loss of accuracy due to the linear approach in this part of the system, vs. stability of the numerical calculations grants adoption of our approach.

3. Results

We carried out a total of 98 simulations with different values of effective thermal diffusivity for the atmosphere and the mantle. In this section, we describe illustrative results. The graphs retain the same color pattern in each panel to identify the time after impact.

In the simulations the thermal diffusivity changes as a function of k_{conv} . It is easier to show the graphs with reference to this coefficient because it represents the number of times that convection is more effective than conduction for each layer (Atmosphere, upper mantle, lower mantle, and core). This allows for a better comparison of how the planet’s cooling might be modified by differences in the rate of heat transfer.

3.1. MAXIMUM TEMPERATURE ENVELOPE

Figure 2 shows the thermal evolution of the planet considering the envelope of maximum temperatures as initial conditions. Four panels are shown, each panel has the axes of temperature on the vertical axis vs Earth’s radius on the horizontal axis. A total of 8 curves are shown in each panel: the two dashed lines are the liquidus and solidus used as reference, the solid black line represents the initial temperatures of the simulation and, the rest of the solid curves represent the temperature profile at various times, as indicated on each panel. Panel a) represents a mantle with weak convection and an atmosphere with very slow heat transfer. It can be observed that the temperature of the atmosphere and mantle decreases slowly.

Under these conditions, the atmosphere receives little heat from the magma ocean and also its heat transmission to outer space is poor. Nevertheless, the liquidus of the magma ocean is reached at the surface much earlier than anywhere else within the interior of the planet. In panel b) the mantle has weak convection, but the atmosphere transmits heat very rapidly. Because the heat flowing from the magma ocean takes longer to distribute from the interior to the surface than the time it takes for heat to travel within the atmosphere, a rapid formation of a solid lithosphere is favored. In panel c) a scenario is shown with a very vigorous mantle convection and an atmosphere that releases heat to space more slowly than it receives it. Under these conditions, the atmosphere heats up and quickly equals the temperature of the planet's surface. Furthermore, the speed at which heat is transmitted inward allows a positive gradient towards the surface and practically the entire planet's

temperature is between the solidus and liquidus curves at the formation of the lithosphere. This layer of solid material serves as a thermal insulator that accumulates liquid material near the surface of the planet. Finally, panel d) shows a vigorous convection in the mantle and an atmosphere that quickly releases heat to outer space. In this case, the conditions for the formation of the lithosphere are met in a short time. However, the transfer of heat from the interior also allows the mantle to cool down enough to begin crystallization from below.

Conditions for the formation of the lithosphere are reached in the four cases before the partial or total crystallization of the planet. Once a lithosphere is formed, the upper layer of the magma ocean becomes relatively insulating because it transmits heat more slowly than the mantle does in its liquid state. Thus, heat flows more slowly outwards and causes the planet to take longer to

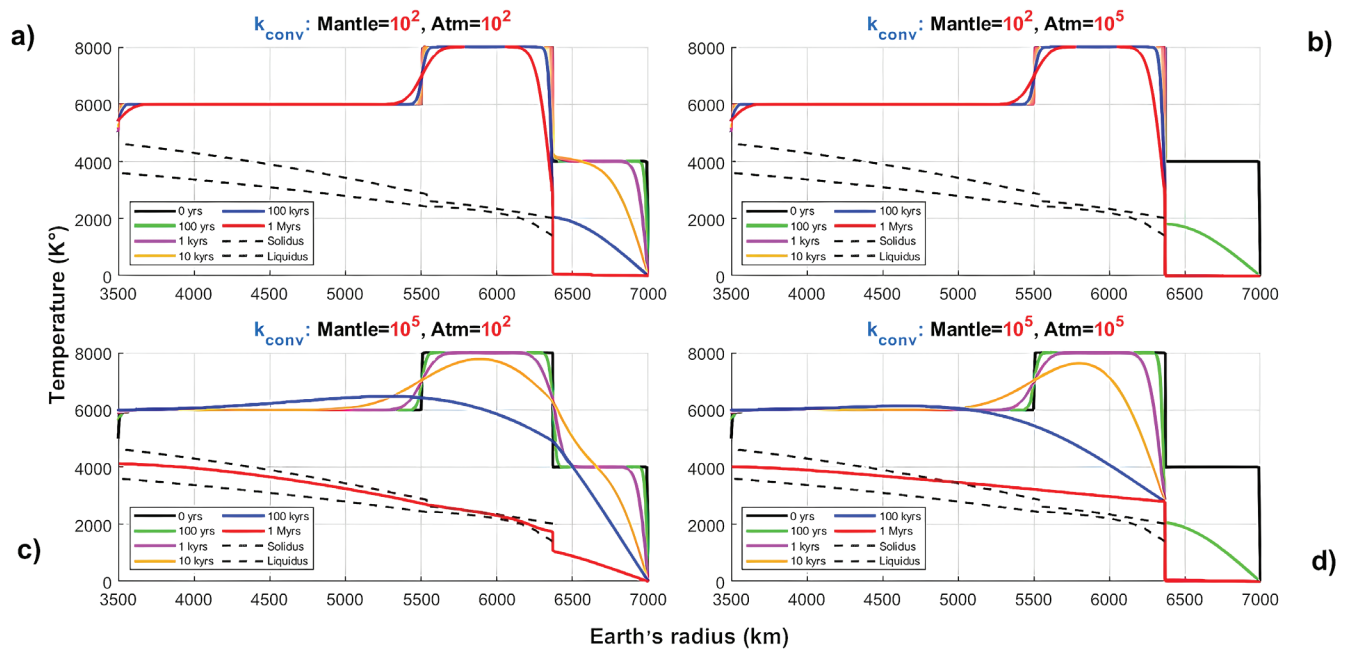


Figure 2 Thermal profiles of the post-impact thermal evolution for initial conditions given by the maximum temperature envelope. Curves of temperature vs radius of the planet are shown in each panel. The dotted black curves delineate the zone where the phase change from liquid to solid takes place. The solid black curves are the initial temperature conditions. Each of the colored curves represents a post-impact cooling time. Four extreme scenarios are shown: a) weak mantle convection and slow heat transfer from the atmosphere to space; b) weak mantle convection and rapid transfer of heat from the atmosphere to space; c) vigorous convection of the mantle and slow transfer of heat from the atmosphere to space; d) vigorous convection of the mantle and rapid transfer of heat from the atmosphere to space.

solidify. In panels a) and b) of Figure 2 the slow heat transfer from the mantle causes surface solidification regardless of how effective the atmosphere is in transmitting heat to space.

3.2. MINIMUM TEMPERATURE ENVELOPE

This section shows cases for the minimum temperatures as initial conditions. To facilitate comparison, the k_{conv} values and color pattern in Figures 2 and 3 are the same. In panel a) the mantle has weak convection and an atmosphere with slow heat transfer. Because the heat flow from the mantle is very low the surface takes a long time to solidify. Nevertheless, we observe that the lithosphere can form while the planet remains in a liquid state. In panel b) the heat transfer in the atmosphere is faster, so the solidification of the surface is more easily achieved while also keeping the planet mostly liquid. When convection is vigorous as in panels c and d, interior temperatures drop rapidly. In these scenarios, the temperatures in the atmosphere are lower than in Figure 2, so the cooling is faster, causing the solidification of the surface,

preserving liquid material inside. This happens regardless of whether the atmosphere exhibits fast or slow heat transfer.

The formation of the lithosphere favors the preservation of a greater part of the mantle in a liquid state for a certain time. This can be easily seen if we compare the blue curves in panels c and d of Figure 3. In c) the planet's surface remains liquid for almost 300000 years while in d) it remains liquid for only 100 years. In either case, the solid lithosphere serves as a relatively insulating layer that keeps heat inside the planet. Although this difference in the amount of liquid material appears to fade over time (red curves in panels c and d of Figure 3), it may be important in the early stages of the planet's solidification.

3.3. TIME OF LITHOSPHERE SOLIDIFICATION

In the previous section, only the extreme scenarios of our 98 simulations were shown. To visualize the results of all our simulations, we concentrate on the estimates of the solidification time yield by each simulation. The surface solidification time is

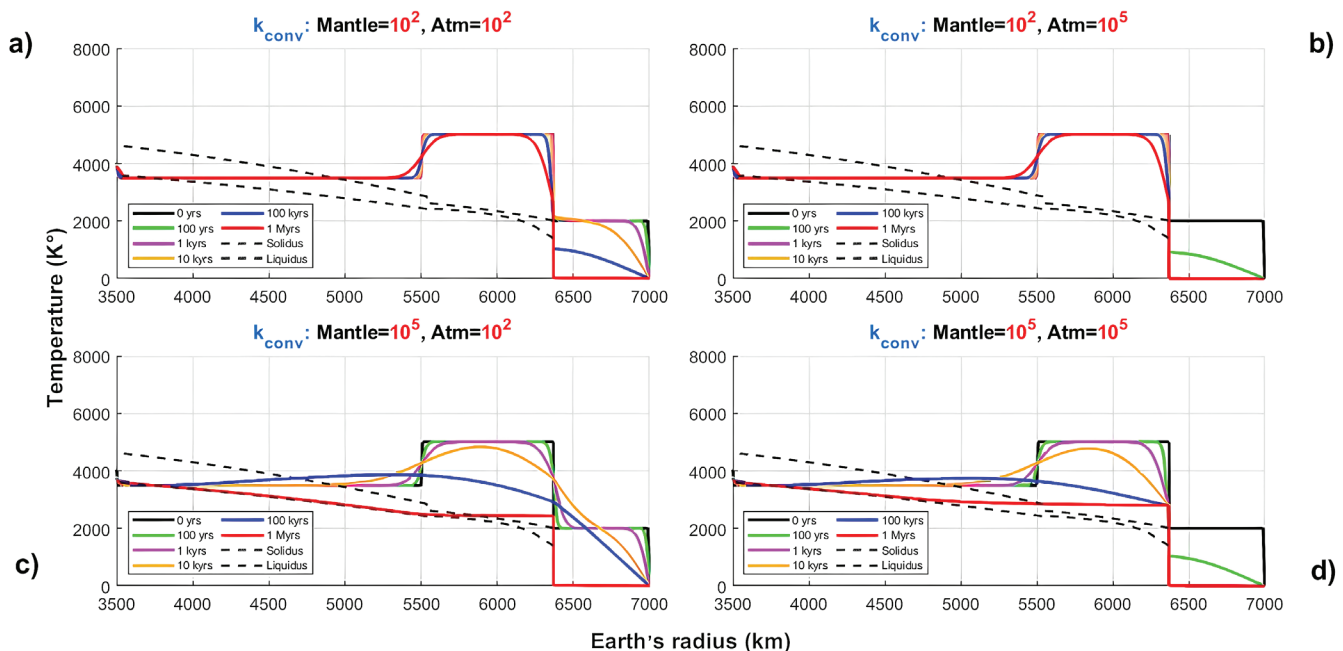


Figure 3 Thermal profiles of the post-impact thermal evolution using the minimum temperature envelope as initial condition. All symbols and panels as in Figure 2.

obtained as the time in which the geotherm drops below the solidus temperature at the surface (1400 K). We also calculated the solidification time of the mantle as the time it takes to reach >90% crystalline material throughout its entire length (*i.e.*, there is no point in the entire mantle with more than 10% liquid material). Although this time of reference does not mark a total solidification in the strictest sense of the word, it suffices to ensure that there are no longer areas of abundant liquid material in the mantle. This also allowed us to reduce the computational calculation time to < 200 Myrs after the impact (in most cases).

In Figure 4 the colors represent the post-impact time of solidification for the lithosphere (upper two diagrams) and for the entire mantle (lower two diagrams). On the horizontal axes are the k_{conv} values for the atmosphere and on the vertical axis are the mantle values for each simulation.

The time of lithosphere formation is shown numerically in years (Figures 4a and 4b; Tables

2 and 3) while millions of years are used for the mantle (Figures 4c and 4d; Tables 2 and 3). The results based on the maximum and minimum temperature envelopes as initial conditions are shown in the left side and right side, respectively. As observed in those diagrams, the effect of the atmosphere is crucial in the first stages of solidification of the planet. It is observed that the formation of the lithosphere occurs rapidly when the k_{conv} value of the atmosphere is $> 10^3$ regardless of the value of the k_{conv} of the mantle. Importantly, even when the time of solidification of the lithosphere may be large, all the simulations indicated that the interior of the magma ocean remained liquid for much longer. Also, the importance of the atmosphere in controlling the speed of cooling of the interior of the planet decreases once the lithosphere has formed.

To establish a clear relationship between the time it takes for the solidification of the mantle and the surface, we calculated their ratio. The

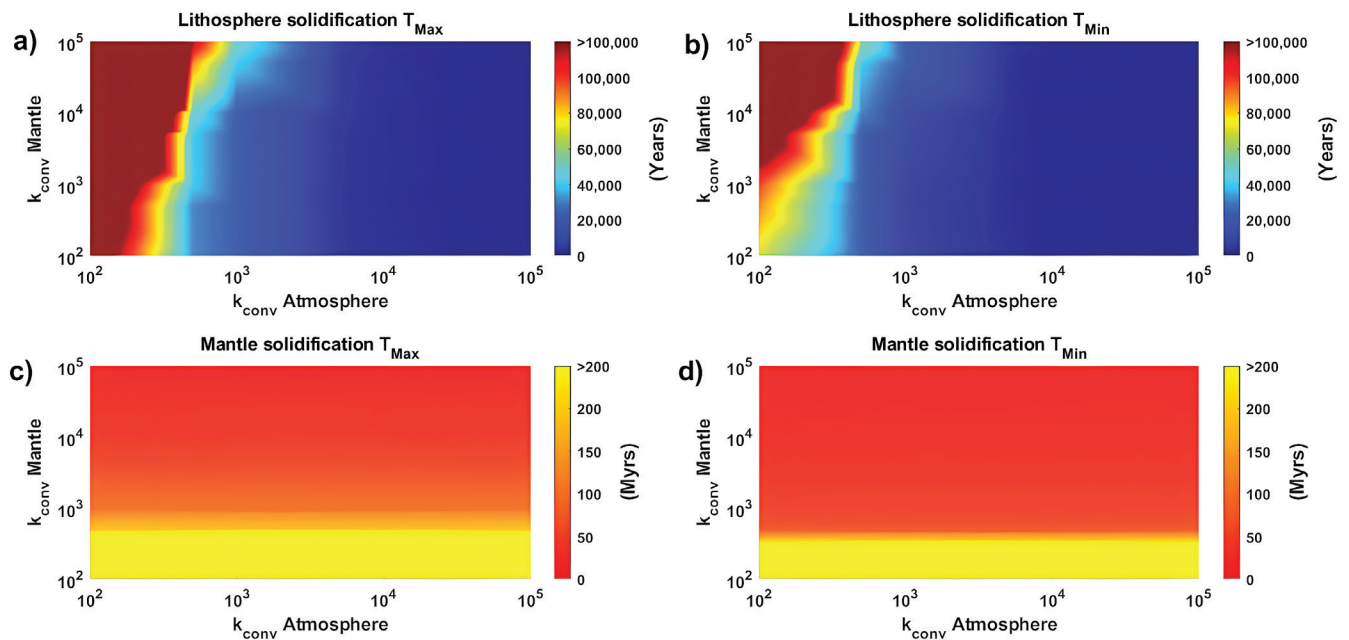


Figure 4 Time of lithosphere solidification as a function of different values of the convective thermal conductivity k_{conv} for the atmosphere and the mantle. Left maximum temperature envelope, right minimum temperature envelope. Above is the solidification time of the lithosphere (a and b), down the solidification time of the mantle (c and d). Data from this picture is reported in Tables 2 and 3.

Table 2. Maximum temperature envelope.

Solidification time of the Lithosphere (Years)		$k_{convective}$ Atmosphere							Solidification time of the Mantle (Myrs)
		10^2	5×10^2	10^3	5×10^3	10^4	5×10^4	10^5	
$k_{convective}$ Mantle	10^2	150000	30000	20000	3000	2000	300	200	>1000
	5×10^2	170000	30000	20000	3000	2000	300	200	189-190
	10^3	190000	40000	20000	3000	2000	300	200	94-95
	5×10^3	320000	40000	20000	3000	2000	300	200	39-40
	10^4	430000	50000	20000	4000	2000	300	200	25-27
	5×10^4	790000	90000	40000	4000	2000	300	200	12-13
	10^5	940000	120000	50000	5000	2000	400	200	5-6

Table 3. Minimum temperature envelope.

Solidification time of the Lithosphere (Years)		$k_{convective}$ Atmosphere							Solidification time of the Mantle (Myrs)
		10^2	5×10^2	10^3	5×10^3	10^4	5×10^4	10^5	
$k_{convective}$ Mantle	10^2	70000	20000	7000	2000	600	200	100	662-663
	5×10^2	90000	20000	7000	2000	700	200	100	65-66
	10^3	100000	20000	7000	2000	700	200	100	34-35
	5×10^3	150000	20000	9000	2000	700	200	100	19-20
	10^4	200000	30000	10000	2000	700	200	100	15-16
	5×10^4	350000	40000	20000	2000	900	200	100	9-10
	10^5	400000	60000	20000	3000	1000	200	100	4-5

Solidification Time Ratio shown in Figure 5 is thus defined as the time of the mantle solidification divided by the time of surface solidification. Low values of this ratio imply that the mantle solidified very shortly after the formation of the lithosphere; higher values indicate that the planet's interior remained liquid for a greater amount of time.

In Figure 5 we can see that the simulations with a higher solidification time ratio ($> 10^4$) have the lowest values of k_{conv} for the mantle and the highest values for the atmosphere. These are the best conditions for the rapid formation of the lithosphere. In contrast, the lowest values in Figure 5 (Solidification time ratio < 100) are found with a vigorous convection of the mantle and an atmosphere that transports heat very slowly.

These conditions are the least favorable for the rapid formation of the lithosphere. Nevertheless, it must be noted that all values of the solidification time ratio in Figure 5 are much larger than unity, which indicates that in all our simulations a solid surface formed before the solidification of the mantle.

In Tables 2 and 3 the left panel shows the lithosphere solidification times (expressed in years) as a function of convective coefficient of thermal conductivity. In the right and with italics, mantle solidification times (expressed in million years) as a function of the convective coefficient of thermal conductivity. The highest and lowest value of k_{conv} of the atmosphere was used to encompass the time range that was calculated for mantle solidification.

4. Discussion

Cooling of the magma ocean could only occur towards outer space through the layer of gas that covers the planet. It should be noted that the radiation emitted by the Earth during the magma ocean phase was much greater than that constantly received by the young Sun. This cooling generates a thermal imbalance in the heat flow until a temperature close to planetary equilibrium is reached. This equilibrium temperature is below the solidification temperature of the surface since otherwise there would have been no cooling. The presence of volatile greenhouse elements in the post-impact atmosphere can prolong the life of the magma ocean (Abe, 1993; Elkins-Tanton, 2012).

However, the amount of volatiles present and the time it takes for degassing the mantle is uncertain (Salvador and Samuel, 2023). If we consider that the greenhouse effect of gases is directly linked to the solidification time, as numerous models have established (Abe, 1993; Lebrun *et al.*, 2013; Zhang *et al.*, 2022), we can assume that the heat flow that

we model implicitly carries the imbalance between outgoing and incoming radiation. The adopted strategy therefore provides a physically reasonable first-order approximation that bypasses the complexity of modeling in detail the convection and radiation of the cooling Earth.

Using different heat transfer rates from the magma ocean to the atmosphere, we have determined times of the start of the formation of the lithosphere. The simulations allowed us to establish some simple relationships between the modeled values and the thermal evolution of the planet. The rapid transmission of heat in the atmosphere favors the rapid solidification of the planet's surface and the existence of liquid material inside during its formation. The slow transmission of heat in the atmosphere prolongs the life of the magma ocean and causes the decrease of liquid material remaining at the time of formation of the lithosphere. Slow convection of the mantle allows the lithosphere to form more easily than vigorous convection. The initial temperature conditions have a great influence on the total solidification

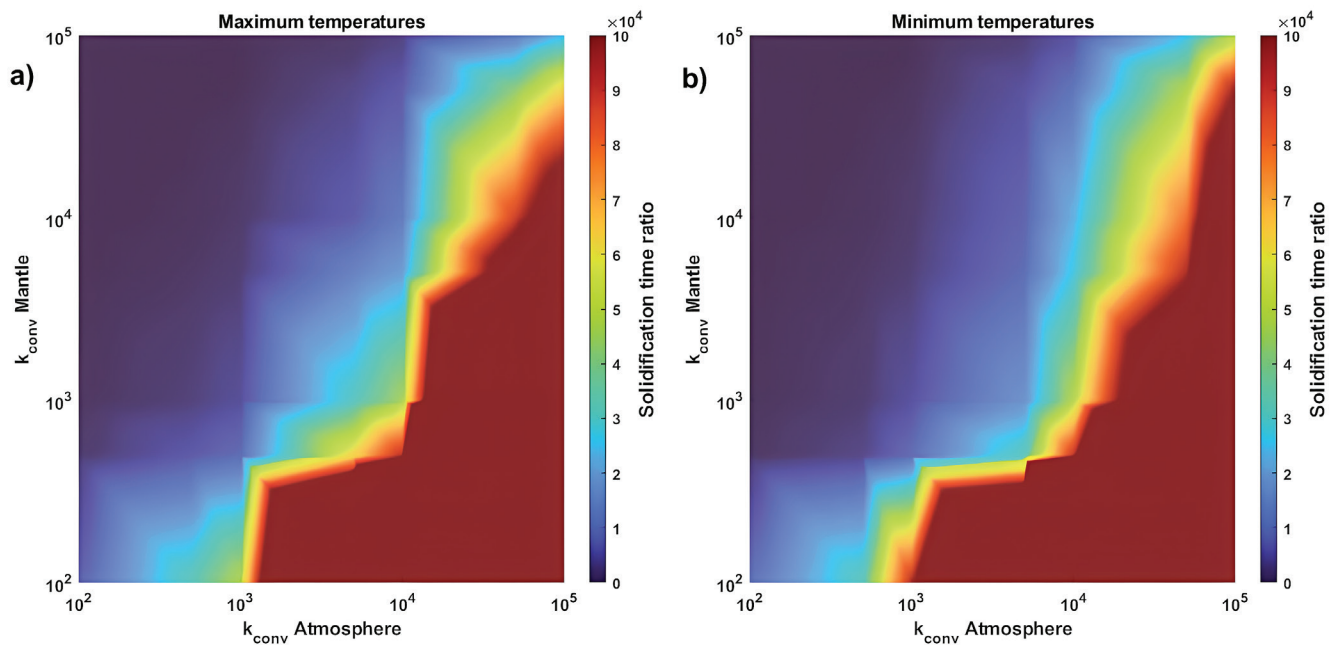


Figure 5 In the left panel we have the simulations for maximum temperatures and on the right side those for minimum temperatures for the Solidification time ratio. The values are the product of the division between the time it takes to completely solidify the mantle and the time it takes to form the lithosphere.

of the mantle because the times of solidification associated with maximum temperatures exceed the times associated with minimum temperatures by several million years. This is best observed by comparing the values of mantle solidification times in Tables 2 and 3. Our results also show a clear dependence between the heat the atmosphere could emit to outer space and the heat that comes from the magma ocean. The contrast between the thermal properties of the atmosphere and the magma ocean therefore has a strong influence on the solidification of the lithosphere.

Our results suggest that there are three main possible evolutionary trends:

1. A magma ocean cooling from below, which has been assumed in many previous studies (Elkins-Tanton, 2012; Lebrun *et al.*, 2013; Nikolaou *et al.*, 2019; Solomatov, 2015; Zhang *et al.*, 2022).

2. An alternative scenario in which the lithosphere can be formed from the top moving downwards (Figures 2a and 2b).

3. A hybrid scenario where solidification occurs both from the surface and from the base of the mantle almost simultaneously. The hybrid scenarios predominate in our simulations (*e.g.* Figures 3a-3d).

A schematic illustration of these evolutionary trends is shown in Figure 6. It is important to highlight that the only possible trend that was not found in our simulations was scenario Figure 6a. In principle, by including a more resistive atmosphere in the models (low k_{conv}) these results could be achieved. Nevertheless, it must be noted that the lower limit of heat transfer (k_{conv}) modeled in this work already has a very low value. Therefore, an atmosphere capable of maintaining the liquid surface until the complete solidification of the mantle requires a heat transfer similar to that presented by some solid metals (Incropera *et al.* 2007; Lienhard and Lienhard, 2008; Çengel, 2006). Such conditions are difficult to achieve in an atmosphere with a composition likely to have been present on the early Earth.

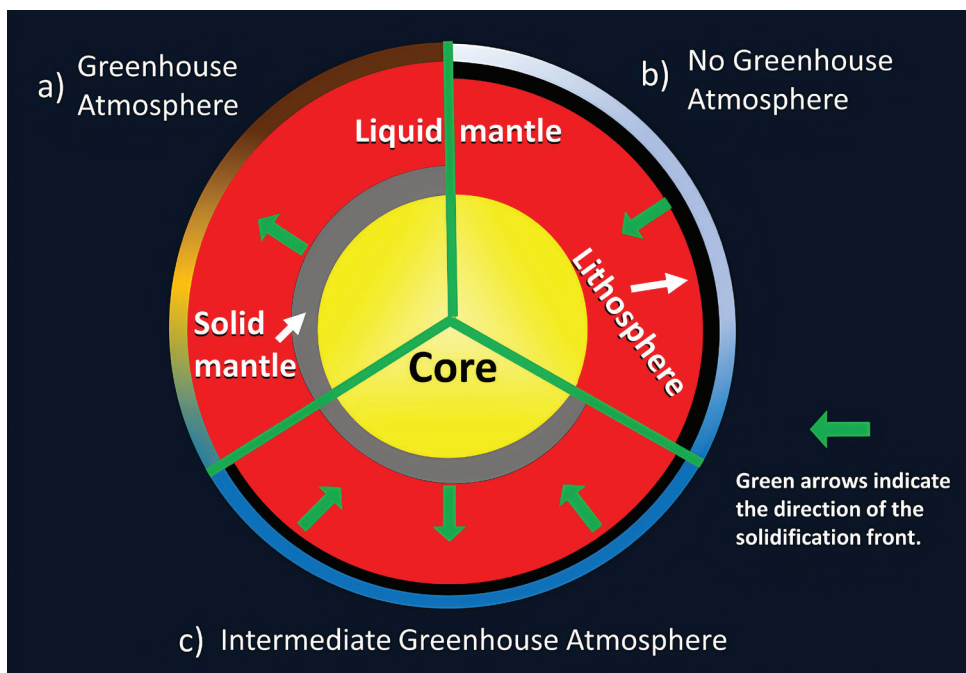


Figure 6 An illustration of the possible evolutionary trends is shown. a) atmosphere with a very powerful greenhouse effect that only allows solidification from the inside. The surface of the planet remains liquid until the mantle is almost completely solidified. b) non-existent or very thermally weak atmosphere that allows rapid solidification of the surface. Solidification of the mantle begins from above. c) the atmosphere is an intermediate point between scenarios a and b, the planet solidifies from both fronts. This is the dominant evolutionary trend in our simulations.

Despite this, the difference in surface solidification time does not have as much impact on the solidification of the interior as the formation of the lithosphere. That is, the formation of the lithosphere occurs before the complete solidification of the mantle regardless of the speed at which the atmosphere transmits heat to space. Therefore, the solidification of the planet's interior can be modified by the appearance of an insulating layer such as the lithosphere.

4.1. ATMOSPHERE AFTER THE GIANT IMPACT

Normally, it is considered that the degassing of the magma ocean produced the greenhouse gases that kept the magma ocean on the planet's surface. Nevertheless, the formation of a proto lithosphere can limit the outward flow of heat, which would lead to increasingly cold climatic conditions. Thus, if the outgassing did not take place quickly, the rapid cooling of the atmosphere could have caused the formation of the lithosphere before the mantle outgassed (Scenarios b and d of Figures 2 and 3). The chemical evolution of the atmosphere therefore, would not have included the release of greenhouse gases, and further cooling from the top of the magma ocean would have been promoted. On the other hand, if the magma ocean can get rid of its volatiles quickly, the greenhouse gas content in the atmosphere would increase. As our results show (Scenario c in Figures 2 and 3), this would become a positive feedback process in which the magma ocean causes the atmosphere to maintain its insulating condition and lengthens the lifetime of the magma ocean. The evidence of liquid water on the planet's surface from zircons and the existence of life suggest that this path was not followed by Earth (Wilde *et al.*, 2001). However, this process could have been followed by Venus. The difference between Earth and Venus, could have been an order of magnitude in the heat transfer from the atmosphere to outer space in the beginning of the magma ocean cooling. Potentially the difference in the solar radiation received by the two planets could have contributed to their

different evolutions of those two planets (Hamano *et al.*, 2013).

It is remarked that the formation of the Earth's atmosphere is a difficult problem still to be solved. The atmosphere could have formed from planetary accretion before the dissipation of the solar nebula, so it could have acquired a nebular composition. It may also have been formed by outgassing from accretional impacts during the creation of proto-Earth (Ahrens *et al.*, 1989; Zahnle *et al.*, 1988). A third possibility is that it could be a product of the degassing of the magma ocean after the impact that gave rise to the Moon (Elkins-Tanton, 2012). In addition, it could have originated from the outgassing of cometary impacts in its last phase of accretion after the giant impact (Wetherill, 1980). Finally, it could have been the result of a random combination of all the processes that have been mentioned. Although there is isotopic evidence supporting each of the different possibilities, it is difficult to encompass all of them in a single model (Pollack and Yung, 1980).

One of the reasons why the argument has been made for a strong greenhouse atmosphere is because of the faint young Sun problem (Zahnle *et al.*, 2010). If the solar radiation in the early years of the Earth was weaker than it is today, a greenhouse effect of the atmosphere would have been necessary to allow the formation of liquid water. This forces us to explain the capture of all the CO₂ that potentially formed that powerful atmosphere to initiate habitable climatic conditions. Furthermore, it is necessary to consider that liquid water on the surface can only form in certain proportions of H₂O and CO₂ (Miyazaki and Korenaga, 2022b). Some zircons from 4.4 Gyrs ago point to the existence of continental lithosphere and liquid water on the planet's surface (Wilde *et al.*, 2001). The appropriate climatic conditions had to be reached quickly. Therefore, the capture of all the CO₂ must have been equally fast. Charnay *et al.* (2020) mention that the explanation may be related to the effect of the atmosphere moderately rich in CO₂, potentially helped by additional warming processes. Although he does not express

it directly, in the presence of higher heat flow to the surface a smaller amount of greenhouse gases will be necessary for the formation of liquid water on the surface. This scenario would fall on the cases shown in Figures 3c and 4c.

Also, there are several reasons to consider scenarios of an evolving Earth without a post-impact atmosphere (e.g., Wang *et al.*, 2022 and references therein). The depletion of rare gases in Earth's atmosphere compared to cosmic abundances indicates that any primary atmosphere must have been lost (Kasting, 1993). The Earth was able to obtain a mass capable of retaining an atmosphere perhaps until after the dissipation of the solar cloud, suggesting that accretion probably occurred mostly in a gas-free environment (Canuto *et al.*, 1983). On the other hand, the "boil-off" theory has been proposed in which the sudden disappearance of the solar nebula could expand the primordial atmosphere and then undergo an efficient escape (Owen and Wu, 2016; Wang *et al.*, 2022). Although part of the primary atmosphere (nebular atmosphere) had survived, it must have been subjected to a lot of accretional impacts that could have eroded it (Chen and Ahrens, 1997). For some simulations the estimated atmosphere loss fraction for the giant impact is only 20% (Genda and Abe, 2003). In the canonical Moon-forming impact, only around 10% of the atmosphere would have been lost from the immediate effects of the collision (Kegerreis *et al.*, 2020). Nevertheless, there are certain conditions that can increase the loss of the atmosphere. For example, the existence of an ocean of water before the impact could amplify the loss of atmosphere and volatiles during the collision (Genda and Abe, 2003). In addition, the thermal consequences of the impact can reduce the atmospheric mass between 50 and 100% for impactors with 10% of the mass of the planet (Biersteker and Schlichting, 2019). Although this is applicable for H/He dominated atmospheres that expand thermally on impact, this type of atmosphere is what one might expect to exist before the end of Earth's accretion. Something that must be considered is that an impact capable of causing the

loss of the atmosphere would inevitably also cause the loss of crust or part of the mantle (Denman *et al.*, 2020). In any case, there is enough evidence justifying the assessment of an evolutionary trend that does not include a highly insulating post-impact atmosphere. As shown by panels b and d of Figures 2 and 3, this scenario inevitably triggers the formation of a lithosphere before the complete solidification of the mantle.

It should be noted that the solidification of the lithosphere before the complete solidification of the mantle does not prevent the formation of the atmosphere. Volcanic degassing (Tajika, 1998; Gaillard *et al.*, 2021), meteoric impact and the process of intrusive magmatism has a strong influence on the total degassing into the atmosphere of the early Earth (Vulpius and Noack, 2022). A more gradual development of the atmosphere would also gradually change the rate at which heat is transferred on this layer. Although this possibility should be kept in mind, given the wide range of conditions upon which the top of the magma ocean cooled before its interior parts, such gradual evolution of the atmosphere would not modify the main trends reported in Figures 2 and 3.

If the atmosphere does not form immediately after the impact, or if it is not as insulating, it would favor the formation of the lithosphere. If there is an insulating atmosphere, but not enough to transport heat more slowly than the magma ocean does, the conditions to form the lithosphere would also have been reached. If turbulent convection of magma ocean favored lateral movements instead of vertical ones as shown by some experimental evidence (Davaille and Limare, 2007), the lithosphere would also form before the total solidification of the planet. Water vapor degassing may not be as abundant as previously speculated (Miyazaki and Korenaga, 2022a). This is an important greenhouse gas, so the atmosphere was possibly less insulating. Even if we consider the large-scale circulation of the mantle, total degassing could have taken longer times than those considered by some previous models (Salvador and Samuel, 2023).

4.2. MAGMA OCEAN CONVECTION

The magma ocean just after the impact is expected to have had a very turbulent, poorly organized, and not large-scale convection. Therefore, the heat transfer could be carried out in a chaotic manner and not as organized as has been proposed until now (Elkins-Tanton, 2012; Solomatov, 2015; Lebrun *et al.*, 2013). This implies that heat transfer can be very different even for nearby points in the planet's interior during this chaotic period. The flow of heat that would come out of the planet's surface has been speculated to reach extremely high amounts (Elkins-Tanton, 2012; Solomatov, 2015). This assumes vigorous convection capable of creating a large-scale circulation that could move large amounts of material from the planet's interior very quickly. But a turbulent convection could decrease the total heat flux reaching the surface of the magma ocean (Davaille and Limare, 2007). Within that context, it is important to mention that our results show a clear relationship between the rate of mantle heat transfer and surface solidification.

The main argument for assuming a magma ocean with a large-scale circulation is based on the Rayleigh number (Solomatov, 2015). Although this dimensionless number can be useful for different modeling, it is important to note that it is not directly applicable to systems with co-existing solids and fluids (Hofmeister, 2020). If we consider this, there is a possibility that large-scale circulation was not as rapid or as vigorous as has been thought. As shown by our results, the lithosphere could form even if large-scale convection in the mantle exists.

4.3. COMPARISON WITH PREVIOUS MODELS

A methodology recurrently used to model the solidification of the magma ocean is described by Solomatov (2015). In his work he considered that the magma ocean behaves as an adiabatic system from the beginning. This is equivalent to a magma ocean that presents a large-scale circulation throughout the entire portion of molten mate-

rial. Almost simultaneously, due to the imposed convection, the mantle degasses until it forms an atmosphere made up mainly of CO₂ and H₂O. This atmosphere must have had an incredibly strong greenhouse effect to keep the planet's surface completely liquid. Such initial conditions are certainly contrasting with the results of SPH simulations for large impacts (Canup, 2008; Carter *et al.*, 2020). One of the main differences between the behavior of the adiabatic curves and the results of the SPH simulations is found in the surface of the planet, where the temperature can be higher due to secondary impacts (*e.g.*, Carter *et al.*, 2020). This makes it difficult to consider an adiabatic curve as an initial condition without explaining how it arrived at.

In addition to the assumed shape of adiabatic curves, there are other implications of the assumed vigorous convective mantle. There are numerous simulations where the planet solidifies in the same way regardless of whether an atmosphere exists or not (*e.g.*, Lebrun *et al.*, 2013). This implies that the model is being forced to have a vigorous convection even without having a greenhouse atmosphere that causes thermal insulation. Adiabatic behavior depends on the insulating boundaries that allow vigorous convection (Incropera *et al.*, 2007; Lienhard and Lienhard, 2008; Çengel, 2006). In contrast, in the different simulations shown above the atmosphere is not insulating enough to prevent the formation of the lithosphere. However, the lithosphere can cause the insulating effect necessary to modify the solidification of the interior. Such dependence on the conditions of the atmosphere seems to be more realistic, as no specific conditions are imposed on the behavior of the mantle in our model.

Furthermore, the physical effect of having a contrast between a gaseous material that distributes and displaces heat better than liquid magma have not been taken into account in previous models. This contrast proves to be extremely important in deciding the rate of cooling of the surface of the magma ocean. Even if we consider that the atmosphere could be preserved as an insulating

system, heat transfer towards outer space would have continued to take place through a much more conductive layer than those representing the mantle-lithosphere. Consequently, no matter how low the viscosity could have been in the post-impact liquid mantle, liquid convection is likely to distribute heat more slowly than the gaseous materials of the atmosphere. Consequently, the conditions for solidification from the top would have been met more easily than those favoring cooling only from the bottom. Therefore, the scenario with two solidification fronts is a very possible scenario for the Earth (Intermediate greenhouse effect).

Finally, it is noted that the lithosphere could have served as an insulating layer, favoring liquid convection in the interior, and storing a greater amount of primordial heat. If the primordial heat did not leave the planet as quickly as thought, this directly impacts geochemical observations (Boyet and Carlson, 2006; Boehnke *et al.*, 2015; Holland *et al.*, 2009), calculations of radiogenic elements in the mantle (KamLAND Collaboration 2011), and our understanding of mantle evolution (Davies, 2007). It could also shed new light on how the Earth's electromagnetic field could have been kept functioning for at least 3.5 Gyrs (Landeau *et al.*, 2022).

5. Conclusions

The most important points that we can highlight from this work are:

- The formation of the lithosphere may be possible before the complete solidification of the magma ocean. Hence, from a purely thermal point of view Earth could have had a magma ocean beneath a solid lithosphere early in its history.
- The formation of a lithosphere could delay the complete cooling of the planet.
- The best conditions for the formation of a lithosphere are reached when the atmosphere transports heat faster than the magma ocean, conditions that are easily met.

Although our model includes many simplifications, it serves as a first approach to the problem posed by the cooling of the planet based on fewer assumptions than many current models. Consequently, our results open the door to possibilities that have not been considered before, but that nonetheless are physically possible and therefore should be explored with attention.

In particular, our approximation shows how the great contrast that exists between the physical properties of the mantle and the atmosphere may have had a great influence on the formation of a lithosphere on the surface of the planet.

Supplementary data

Carapia, M., 2023, Atmospheric_influence_on_lithosphere_formation (Version 1). (Software), figshare. <https://doi.org/10.6084/m9.figshare.24558262>

Contributions of authors

Both authors contributed to the conceptualization, methodology, research, writing of the manuscript, preparation of figures, revision of the manuscript and interpretation of results.

Financing

Financial support from CONAHCYT through grant A1-S-23107 to E. Cañón-Tapia and a scholarship to M. Carapia is acknowledged.

Conflicts of interest

The authors declare that there are no competing interests, financial or otherwise, that could have influenced the reported research.

Handling editor

Antoni Camprubí.

References

- Abe, Y., 1993, Physical state of the very early Earth: *Lithos*, 30(3-4), 223-235. [https://doi.org/10.1016/0024-4937\(93\)90037-D](https://doi.org/10.1016/0024-4937(93)90037-D)
- Ahrens, T.J., O'Keefe, J.D., Lange, M.A., 1989, Formation of atmospheres during accretion of the terrestrial planets, in Atreya, S.K., Pollack, J.B., Matthews, M.S. (eds.), *Origin and Evolution of Planetary and Satellite Atmospheres*: University of Arizona Press, 328–385. <https://doi.org/10.2307/j.ctv20dsb5m.15>
- Biersteker, J.B., Schlichting, H.E., 2019, Atmospheric mass-loss due to giant impacts: the importance of the thermal component for hydrogen–helium envelopes: *Monthly Notices of the Royal Astronomical Society*, 485(3), 4454-4463. <https://doi.org/10.1093/mnras/stz738>
- Boehnke, P., Caffee, M.W., Harrison, T.M., 2015, Xenon isotopes in the MORB source, not distinctive of early global degassing: *Geophysical Research Letters*, 42(11), 4367-4374. <https://doi.org/10.1002/2015GL063636>
- Boyet, M., Carlson, R.W. 2006, A new geochemical model for the Earth's mantle inferred from 146Sm–142Nd systematics: *Earth and Planetary Science Letters*, 250(1-2), 254-268. <https://doi.org/10.1016/j.epsl.2006.07.046>
- Canup, R.M., 2008, Accretion of the Earth. *Philosophical Transactions of the Royal Society A: Mathematical, Physical and Engineering Sciences*, 366(1883), 4061-4075. <https://doi.org/10.1098/rsta.2008.0101>
- Canup, R.M., Esposito, L.W., 1996, Accretion of the Moon from an impact-generated disk: *Icarus*, 119(2), 427-446. <https://doi.org/10.1006/icar.1996.0028>
- Canuto, V. M., Levine, J.S., Augustsson, T.R., Imhoff, C.L., Giampapa, M.S., 1983, The young Sun and the atmosphere and photochemistry of the early Earth: *Nature*, 305(5932), 281-286. <https://doi.org/10.1038/305281a0>
- Carter, P.J., Lock, S.J., Stewart, S.T., 2020, The energy budgets of giant impacts: *Journal of Geophysical Research: Planets*, 125(1), e2019JE006042. <https://doi.org/10.1029/2019JE006042>
- Çengel, Y.A., 2006, *Heat exchangers, Heat and Mass Transfer: A Practical Approach*: McGraw-Hill, 901 p.
- Charnay, B., Wolf, E.T., Marty, B., Forget, F., 2020, Is the faint young Sun problem for Earth solved?: *Space Science Reviews*, 216, 1-29. <https://doi.org/10.1007/s11214-02000711-9>
- Chen, G.Q., Ahrens, T.J., 1997, Erosion of terrestrial planet atmosphere by surface motion after a large impact: *Physics of the Earth and Planetary Interiors*, 100(1-4), 21-26. [https://doi.org/10.1016/S0031-9201\(96\)03228-1](https://doi.org/10.1016/S0031-9201(96)03228-1)
- Ćuk, M., Stewart, S.T., 2012, Making the Moon from a fast-spinning Earth: A giant impact followed by resonant despinning: *Science*, 338(6110), 1047-1052. <https://doi.org/10.1126/science.1225542>
- Davaille, A., Limare, A., 2007, Laboratory studies of mantle convection: *Mantle Dynamics*, 7, 89-165. <https://doi.org/10.1016/B978-044452748-6.00116-4>
- Davies, G.F., 2007, Thermal evolution of the mantle, in Schubert, G. (ed.), *Treatise on Geophysics*: Elsevier, 197-216. <https://doi.org/10.1016/B978-044452748-6.00145-0>
- Denman, T.R., Leinhardt, Z.M., Carter, P.J., Mordasini, C., 2020, Atmosphere loss in planet–planet collisions: *Monthly Notices of the Royal Astronomical Society*, 496(2), 1166-1181. <https://doi.org/10.1093/mnras/staa1623>
- Elkins-Tanton, L.T., 2012), Magma oceans in the inner solar system: *Annual Review of Earth and Planetary Sciences*, 40(113), 2012. <https://doi.org/10.1146/annurev-earth-042711-105503>
- Fiquet, G., Auzende, A.L., Siebert, J., Corgne, A.,

- Bureau, H., Ozawa, H., Garbarino, G., 2010, Melting of peridotite to 140 gigapascals: *Science*, 329(5998), 1516-1518. <https://doi.org/10.1126/science.1192448>
- Gaillard, F., Bouhifd, M.A., Füri, E., Malavergne, V., Marrocchi, Y., Noack, L., Ortenzi, G., Roskosz, M., Vulpius, S., 2021, The Diverse Planetary Ingassing/Outgassing Paths Produced over Billions of Years of Magmatic Activity. *Space Science Reviews*, 217, 22, <https://doi.org/10.1007/s11214-021-00802-1>
- Genda, H., Abe, Y., 2003, Survival of a proto-atmosphere through the stage of giant impacts: the mechanical aspects: *Icarus*, 164(1), 149-162. [https://doi.org/10.1016/S0019-1035\(03\)00101-5](https://doi.org/10.1016/S0019-1035(03)00101-5)
- Goncharov, A.F., Beck, P., Struzhkin, V.V., Haugen, B.D., Jacobsen, S.D., 2009, Thermal conductivity of lower-mantle minerals, 174(1-4), 24-32. <https://doi.org/10.1016/j.pepi.2008.07.033>
- Hamano, K., Abe, Y., Genda, H., 2013, Emergence of two types of terrestrial planet on solidification of magma ocean: *Nature*, 497(7451), 607-610. <https://doi.org/10.1038/nature12163>
- Herzberg, C., Raterron, P., Zhang, J., 2000, New experimental observations on the anhydrous solidus for peridotite KLB-1: *Geochemistry, Geophysics, Geosystems*, 1(11). <https://doi.org/10.1029/2000GC000089>
- Hirschmann, M.M., 2000, Mantle solidus: Experimental constraints and the effects of peridotite Composition: *Geochemistry, Geophysics, Geosystems*, 1(10). <https://doi.org/10.1029/2000GC000070>
- Hofmeister, A.M., Criss, R.E., 2019, The macroscopic picture of heat retained and heat emitted: Thermodynamics and its historical development, in Hofmeister, A.M. (ed.), *Measurements, Mechanisms, and Models of Heat Transport*: Amsterdam, Elsevier, 1-34. <https://doi.org/10.1016/B978-0-12-809981-0.00001-2>
- Hofmeister, A., 2020, Heat transport processes on planetary scales, in Hofmeister, A.M. (ed.), *In Heat transport and energetics of the earth and rocky planets*: Elsevier, 59-88. <https://doi.org/10.1016/C2015-0-06204-9>
- Holland, G., Cassidy, M., Ballentine, C.J., 2009, Meteorite Kr in Earth's mantle suggests a late accretionary source for the atmosphere: *Science*, 326(5959), 1522-1525. <https://doi.org/10.1126/science.1179518>
- Incropera F.P., Dewitt. D.P., Bergman, T.L., Lavine, A.S., 2007, *Fundamentals of Heat and Mass Transfer*: London, John Wiley & Sons, 997 p.
- KamLAND Collaboration, 2011, Partial radiogenic heat model for Earth revealed by geoneutrino measurements: *Nature Geoscience*, 4(9), 647-651. <https://doi.org/10.1038/ngeo1205>
- Kasting, J.F., 1993, Earth's early atmosphere: *Science*, 259(5097), 920-926. <https://doi.org/10.1126/science.11536547>
- Kegerreis, J.A., Eke, V.R., Massey, R.J., Teodoro, L.F.A., 2020, Atmospheric erosion by giant impacts onto terrestrial planets: *The Astrophysical Journal*, 897(2), 161. <https://doi.org/10.3847/1538-4357/ab9810>
- Labrosse, S., Hernlund, J.W., Coltice, N., 2007, A crystallizing dense magma ocean at the base of the Earth's mantle: *Nature*, 450(7171), 866-869. <https://doi.org/10.1038/nature06355>
- Landeau, M., Fournier, A., Nataf, H.C., Cébron, D., Schaeffer, N., 2022, Sustaining Earth's magnetic dynamo: *Nature Reviews Earth & Environment*, 3, 255-269. <https://doi.org/10.1038/s43017-022-00264-1>
- Lebrun, T., Massol, H., Chassefière, E., Davaille, A., Marcq, E., Sarda, P., Leblanc, F. Brandeis, G. (2013). Thermal evolution of an early magma ocean in interaction with the atmosphere: *Journal of Geophysical Research: Planets*, 118(6), 1155-1176. <https://doi.org/10.1002/jgre.20068>
- Lienhard, J.H.I., Lienhard, J.H.V., 2008, Heat conduction concepts, thermal resistance, and

- the overall heat transfer coefficient: A Heat Transfer Textbook, 3, 62. <http://web.mit.edu/lienhard/www/ahtt.html>
- Melchior, P., 1986, The Physics of the Earth's Core, An Introduction: Oxford, New York, Beijing, Frankfurt, Sao Paulo, Sydney, Tokyo, Toronto: Pergamon Press, 256 p. <https://doi.org/10.1016/C2009-0-11041-3>
- Miyazaki, Y., Korenaga, J., 2022a, A wet heterogeneous mantle creates a habitable world in the Hadean: *Nature*, 603(7899), 86-90. <https://doi.org/10.1038/s41586-021-04371-9>
- Miyazaki, Y., Korenaga, J., 2022b, Inefficient water degassing inhibits ocean formation on rocky planets: An insight from self-consistent mantle degassing models: *Astrobiology*, 22(6), 713-734. <https://doi.org/10.1089/ast.2021.0126>
- Monteux, J., Andrault, D., Samuel, H., 2016, On the cooling of a deep terrestrial magma Ocean: *Earth and Planetary Science Letters*, 448, 140-149. <https://doi.org/10.1016/j.epsl.2016.05.010>
- Monteux, J., Andrault, D., Guitreau, M., Samuel, H., Demouchy, S., 2020, A mushy Earth's mantle for more than 500 Myr after the magma ocean solidification: *Geophysical Journal International*, 221(2), 1165-1181. <https://doi.org/10.1093/gji/ggaa064>
- Nakazawa, K., Mizuno, H., Sekiya, M., Hayashi, C., 1985, Structure of the primordial atmosphere surrounding the early-Earth: *Journal of geomagnetism and geoelectricity*, 37(8), 781-799. <https://doi.org/10.5636/jgg.37.781>
- Nikolaou, A., Katyal, N., Tosi, N., Godolt, M., Grenfell, J.L., Rauer, H., 2019, What factors affect the duration and outgassing of the terrestrial magma ocean?: *The Astrophysical Journal*, 875(1), 11. <https://doi.org/10.3847/1538-4357/ab08ed>
- Owen, J.E., Wu, Y., 2016, Atmospheres of low-mass planets: the "boil-off": *The Astrophysical Journal*, 817(2), 107. <https://doi.org/10.3847/0004-637X/817/2/107>
- Pollack, J.B., Yung, Y.L., 1980, Origin and evolution of planetary atmospheres: *Annual Review of Earth and Planetary Sciences*, 8(1), 425-487. <https://doi.org/10.1146/annurev.ca.08.050180.002233>
- Salvador, A., Samuel, H., 2023, Convective outgassing efficiency in planetary magma oceans: insights from computational fluid dynamics: *Icarus*, 390, 115265. <https://doi.org/10.1016/j.icarus.2022.115265>
- Schlichting, H.E., Mukhopadhyay, S., 2018, Atmosphere impact losses: *Space Science Reviews*, 214(1), 1-31. <https://doi.org/10.1007/s11214-018-0471-z>
- Sleep, N.H., Zahnle, K., Neuhoff, P.S., 2001, Initiation of clement surface conditions on the earliest Earth: *Proceedings of the National Academy of Sciences*, 98(7), 3666-3672. <https://doi.org/10.1073/pnas.071045698>
- Solomatov, V., 2015, Magma Oceans and Primordial Mantle Differentiation, in Schubert G.(ed.), *Treatise on Geophysics*: Elsevier, 81-104 <https://doi.org/10.1016/B978-0-444-53802-4.00155-X>
- Suzuki, A., Ohtani, E., 2003, Density of peridotite melts at high pressure. *Physics and Chemistry of Minerals*, 30, 449-456. <https://doi.org/10.1007/s00269-003-0322-6>
- Tajika, E., 1998, Mantle degassing of major and minor volatile elements during the Earth's History: *Geophysical research letters*, 25(21), 3991-3994. <https://doi.org/10.1029/1998GL900106>
- Tonks, W.B., Melosh, H.J., 1993, Magma ocean formation due to giant impacts: *Journal of Geophysical Research: Planets*, 98(E3), 5319-5333. <https://doi.org/10.1029/92JE02726>
- Vulpius, S., Noack, L., 2022, Intrusive magmatism strongly contributed to the volatile release into the atmosphere of early Earth: *Geochemistry, Geophysics, Geosystems*, 23(12), e2021GC010230. <https://doi.org/10.1029/2021GC010230>
- Wang, Z., Zhou, Y., Liu, Y., 2022, The escape

- mechanisms of the proto-atmosphere on terrestrial planets: “boil-off” escape, hydrodynamic escape and impact erosion: *Acta Geochimica*, 41(4), 592-606. <https://doi.org/10.1007/s11631-021-00515-w>
- Wetherill, G.W., 1980, Formation of the terrestrial planets: *Annual review of astronomy and astrophysics*, 18(1), 77-113. <https://doi.org/10.1146/annurev.aa.18.090180.000453>
- Wilde, S.A., Valley, J.W., Peck, W.H., Graham, C.M., 2001, Evidence from detrital zircons for the existence of continental crust and oceans on the Earth 4.4 Gyr ago: *Nature*, 409(6817), 175-178. <https://doi.org/10.1038/35051550>
- Whittington, A.G., 2019, Heat and mass transfer in glassy and molten silicates, in Hofmeister A.M. (ed.), *Measurements, mechanisms, and models of heat transport*: Elsevier, 327-357. <https://doi.org/10.1016/B978-0-12-809981-0.00010-3>
- Zahnle, K.J., 2006, Earth’s earliest atmosphere: *Elements*, 2(4), 217-222. <https://doi.org/10.2113/gselements.2.4.217>
- Zahnle, K., Arndt, N., Cockell, C., Halliday, A., Nisbet, E., Selsis, F., Sleep, N.H., 2007, Emergence of a Habitable Planet: *Space Science Reviews*, 129, 35-78. <https://doi.org/10.1007/s11214-007-9225-z>
- Zahnle, K.J., Kasting, J.F., Pollack, J.B., 1988, Evolution of a steam atmosphere during Earth’s accretion: *Icarus*, 74(1), 62-97. [https://doi.org/10.1016/0019-1035\(88\)90031-0](https://doi.org/10.1016/0019-1035(88)90031-0)
- Zahnle, K., Schaefer, L., Fegley, B., 2010, Earth’s earliest atmospheres: Cold Spring Harbor perspectives in biology, 2(10), a004895. <https://doi.org/10.1101/cshperspect.a004895>
- Zhang, J., Herzberg, C., 1994, Melting experiments on anhydrous peridotite KLB-1 from 5.0 to 22.5 GPa.: *Journal of Geophysical Research: Solid Earth*, 99(B9), 17729-17742. <https://doi.org/10.1029/94JB01406>
- Zhang, Y., Zhang, N., Tian, M., 2022, Internal dynamics of magma ocean and its linkage to atmospheres: *Acta geochimica*, 41(4), 568-591. <https://doi.org/10.1007/s11631-021-00514-x>

Appendix A

A1.1 RADIOGENIC ELEMENTS DURING LITHOSPHERE SOLIDIFICATION

This section shows the impact of the presence of radiogenic elements inside the magma ocean during lithosphere formation. The results of our simulations suggest that lithosphere solidification occurred in less than a million years. Therefore, the temperature difference for some simulations during this period with and without radioactive heat generation has been compared. This has been done by subtracting the temperature of simulations with heat generation by radiogenic elements from the results of the same simulation without them. An average of this difference has been obtained for the entire mantle, since it is here where radiogenic elements are homogeneously distributed.

Figure A1 shows a series of curves representing temperature differences averaged throughout the mantle for simulations of maximum (*solid*) and minimum (*dotted*) temperatures. For simplicity, only some of the simulations performed in this work have been exemplified. The red curves are those with the weakest heat transfer ($k_{conv}=10^2$), the magenta curves have the fastest heat transfer ($k_{conv}=10^5$) and finally, the green ($k_{conv}=10^3$) and blue ($k_{conv}=10^4$) curves are intermediate cases. All curves show a clear upward trend, indicating that the impact of radiogenic elements increases with time. However, the difference between all these simulations is less than 1.5°K for the first million years. In other words, the temperature difference between considering the influence of radiogenic heat production and neglecting it, is less than 0.1% of the solidification temperature considered in this work (1400 °K).

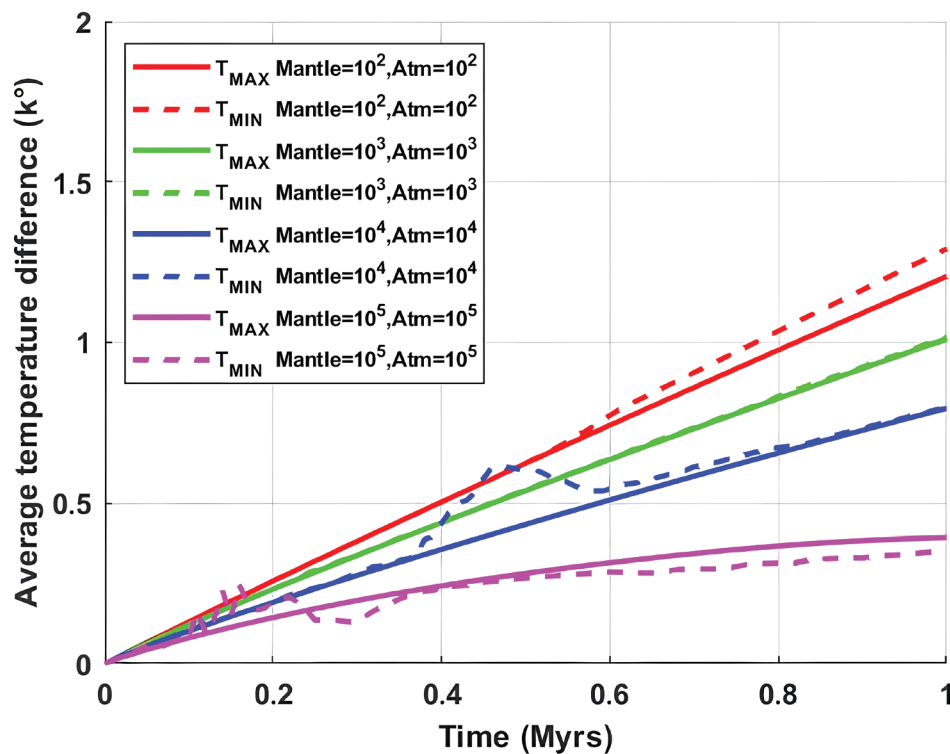


Figure A1 A series of curves representing the average temperature difference for the mantle. The temperature difference was obtained between simulations with identical initial parameters, only distinguished by the presence of radiogenic elements. These differences have been averaged for the entire mantle over time. The solid curves represent the maximum initial temperatures and the dashed curves the minimum initial temperatures.